Pictorial Essay | Musculoskeletal Imaging

https://doi.org/10.3348/kjr.2018.19.6.1147
pISSN 1229-6929 · eISSN 2005-8330
Korean J Radiol 2018;19(6):1147-1160

Korean Journal of Radiology
KJR

Imaging Features of Soft-Tissue Calcifications and Related Diseases: A Systematic Approach

Zhen-An Hwang, MD[1, 2], Kyung Jin Suh, MD, PhD[3], Dillon Chen, MD[4], Wing P. Chan, MD[1, 2], Jim S. Wu, MD[5]

[1]Department of Radiology, Wan Fang Hospital, Taipei Medical University, Taipei 116, Taiwan; [2]Department of Radiology, School of Medicine, College of Medicine, Taipei Medical University, Taipei 110, Taiwan; [3]Department of Radiology, Dongguk University Gyeongju Hospital, Gyeongju 38067, Korea; [4]Department of Radiology, University of California, Davis, CA 95817, USA; [5]Department of Radiology, Beth Israel Deaconess Medical Center, Boston, MA 02215, USA

Soft-tissue calcification refers to a broad category of lesions. Calcifications are frequently identified by radiologists in daily practice. Using a simple algorithm based on the distribution pattern of the lesions and detailed clinical information, these calcified lesions can be systematically evaluated. The distribution pattern of the calcific deposits enables initial division into calcinosis circumscripta and calcinosis universalis. Using laboratory test results (serum calcium and phosphate levels) and clinical history, calcinosis circumscripta can be further categorized into four subtypes: dystrophic, iatrogenic, metastatic, and idiopathic calcification. This pictorial essay presents a systematic approach to the imaging features of soft-tissue calcifications and related diseases.

Keywords: *Calcification; Radiograph; Soft tissue*

INTRODUCTION

Soft-tissue calcification is a broad category of lesions that are frequently found by radiologists in daily practice. Using a simple algorithm based on distribution patterns, combined with detailed clinical information, such as history and laboratory testing, soft-tissue calcifications can be systematically evaluated. Calcinosis is a condition characterized by deposition of calcium in the skin, subcutaneous tissue, muscles, or visceral organs. This classification algorithm begins with the distribution pattern of the calcific deposits (Fig. 1) into one of two forms: calcinosis universalis or calcinosis circumscripta.

Received October 23, 2017; accepted after revision May 8, 2018.
Corresponding author: Wing P. Chan, MD, Department of Radiology, Wan Fang Hospital, Taipei Medical University, 111 Hsing-Long Road, Section 3, Taipei 116, Taiwan.
• Tel: (8862) 29307930 • Fax: (8862) 2916809
• E-mail: wingchan@tmu.edu.tw

Calcinosis Universalis

Calcinosis universalis, also termed "dermal calcinosis" or "diffuse interstitial calcinosis," is defined as diffuse deposition of calcium in the skin, subcutaneous cellular tissue, tendons, or muscles (1). The exact pathogenesis of calcinosis deposition remains unknown; however, it may be an intracellular accumulation of calcium secondary to an altered cellular membrane due to trauma or inflammation (2). Calcinosis universalis is a recognized presentation of connective tissue diseases, especially in juvenile dermatomyositis and polymyositis (3). Juvenile dermatomyositis accounts for up to 40% of these lesions; they are less common in adult-onset dermatomyositis,

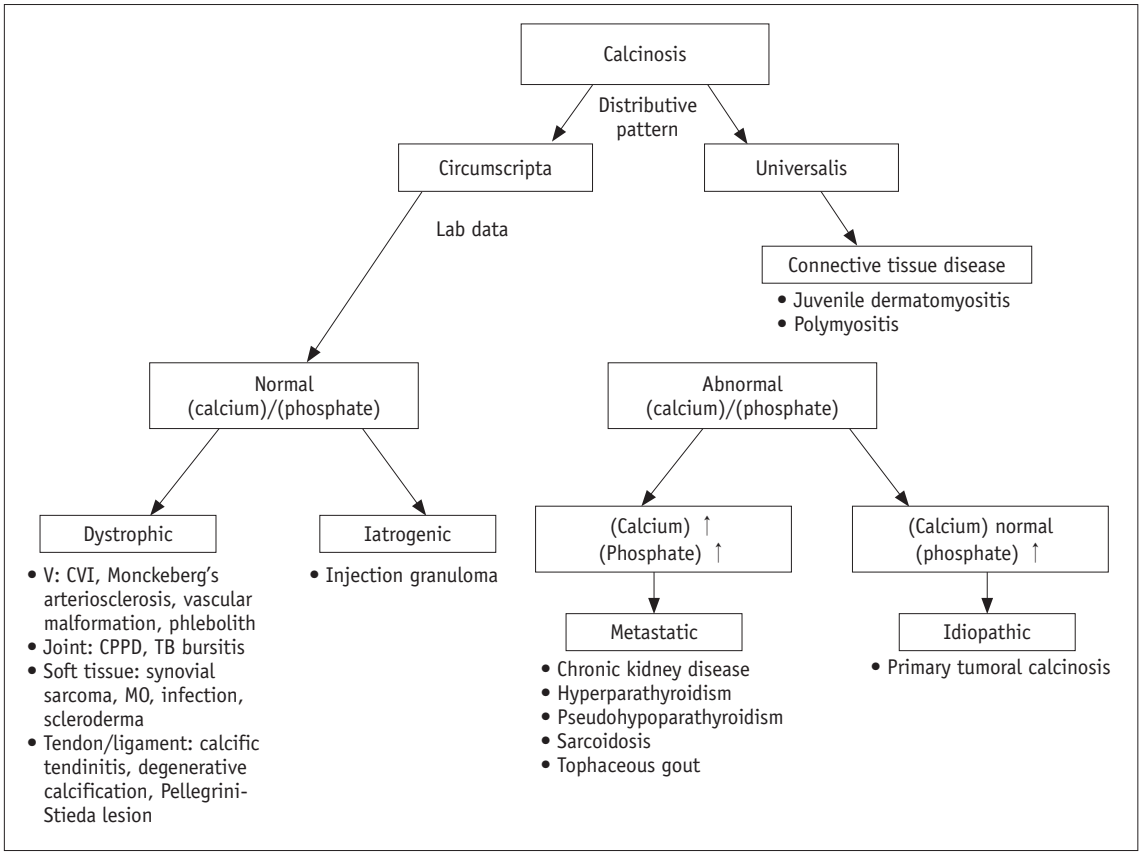

Fig. 1. Evaluation flowchart enabling division of calcified lesions into calcinosis circumscripta and calcinosis universalis based on distribution patterns. Using laboratory testing, calcinosis circumscripta can be categorized into dystrophic, iatrogenic, metastatic, and idiopathic calcification subtypes. CPPD = calcium pyrophosphate dihydrate crystal deposition, CVI = chronic venous insufficiency, MO = myositis ossificans, TB bursitis = tuberculous bursitis, V= vascular

which accounts for 10% (2, 4). Radiographically, they feature extensive sheet-like distributions of calcification (Fig. 2) (3).

Calcinosis Circumscripta

Calcinosis circumscripta manifests as localized or isolated calcification. According to serum levels of calcium and phosphate, these lesions can be further categorized into dystrophic, iatrogenic, metastatic, and idiopathic subtypes (Fig. 1). Dystrophic calcification is defined as calcification in altered necrotic tissue resulting from an underlying inflammatory process. It occurs in patients whose serum calcium and phosphorus levels are normal (5). Iatrogenic calcification results from a previous procedure or treatment such as repeated injections.

When soft-tissue calcification occurs with an elevated serum calcium-phosphorus ion product, it is known as metastatic calcification. In these cases, amorphous calcium phosphate and calcium hydroxyapatite crystals are deposited in multiple locations including the visceral organs (5). Idiopathic calcification is associated with a normal serum calcium level but elevated phosphate levels (6). Primary tumoral calcinosis is a hereditary metabolic dysfunction of phosphate regulation associated with massive periarticular calcinosis (3).

Dystrophic Calcification

Depending on the involved locations, dystrophic calcification can be grouped into the following causes: vascular-related (chronic venous insufficiency, Mönckeberg's arteriosclerosis, phleboliths and venous malformation); joint-related (calcium pyrophosphate deposition disease, tuberculous trochanteric bursitis); soft-tissue related (synovial sarcoma, myositis ossificans [MO], parasitic infection, connective tissue disease); and tendon/ligament-related (degenerative calcification, calcific tendinitis, and Pellegrini-Stieda lesion/syndrome) (Fig. 1).

Korean Journal of Radiology
KJR

Fig. 2. Calcinosis universalis in 56-year-old man with dermatomyositis who presented with longstanding skin and muscle pain. Coronal computed tomography image reveals calcinosis universalis, in which extensive calcification (arrowheads) is distributed in sheet-like pattern in bilateral gluteal regions and lower extremities.

Fig. 3. CVI in 93-year-old woman with ulcer on her left leg. Anteroposterior radiograph of knee reveals characteristic trabecular calcification (arrow) at medial aspect of left tibia resulting from CVI. CVI = chronic venous insufficiency

Vascular Disease-Related Calcifications

Chronic Venous Insufficiency

Chronic venous insufficiency manifests as variable cutaneous findings including varicose veins, edema, hyperpigmentation, ulcerations and, occasionally, subcutaneous calcification. Two patterns of calcification are encountered on plain radiographs: punctate and trabecular/reticular types (Fig. 3) (7). The incidence of calcification correlates with disease duration and severity. Patients with longer disease duration present primarily with the trabecular type (7). Besides, the presence of these calcification causes poor wound healing. In addition, wavy and irregular periosteal reactions (Fig. 4) secondary to increased mean interstitial fluid pressure is occasionally found to exert pressure on the periosteum (8).

Mönckeberg's Arteriosclerosis

Two forms of arterial calcifications due to aging are recognized on radiography: those of the arterial intima (atherosclerosis); and those of the tunica media (Mönckeberg's arteriosclerosis) (9). Mönckeberg's arteriosclerosis refers to medial calcification deposits in the medium and small muscular arteries of the lower limbs and do not cause luminal narrowing. Currently, the exact etiology of this type of atherosclerosis remains unclear; they are primarily incidental findings that appear as a "railroad track" pattern (Fig. 5) (10).

Phleboliths

Phleboliths refer to calcifications within venous structures. They are usually characterized by spherical or round nodular shapes (Fig. 6).

Venous Malformations

Vascular malformations are categorized as low-flow malformations (venous, lymphatic, capillary, capillary-venous, and capillary-lymphatic-venous) or high-flow malformations (arteriovenous malformations and arteriovenous fistulas) (11). They are the most common peripheral vascular malformations, and occur in the head and neck (40%), trunk (20%), and extremities (40%) (11, 12). They are frequently incorrectly referred to as "cavernous hemangiomas." On magnetic resonance (MR) images, they usually present as septated or tubular lesions with

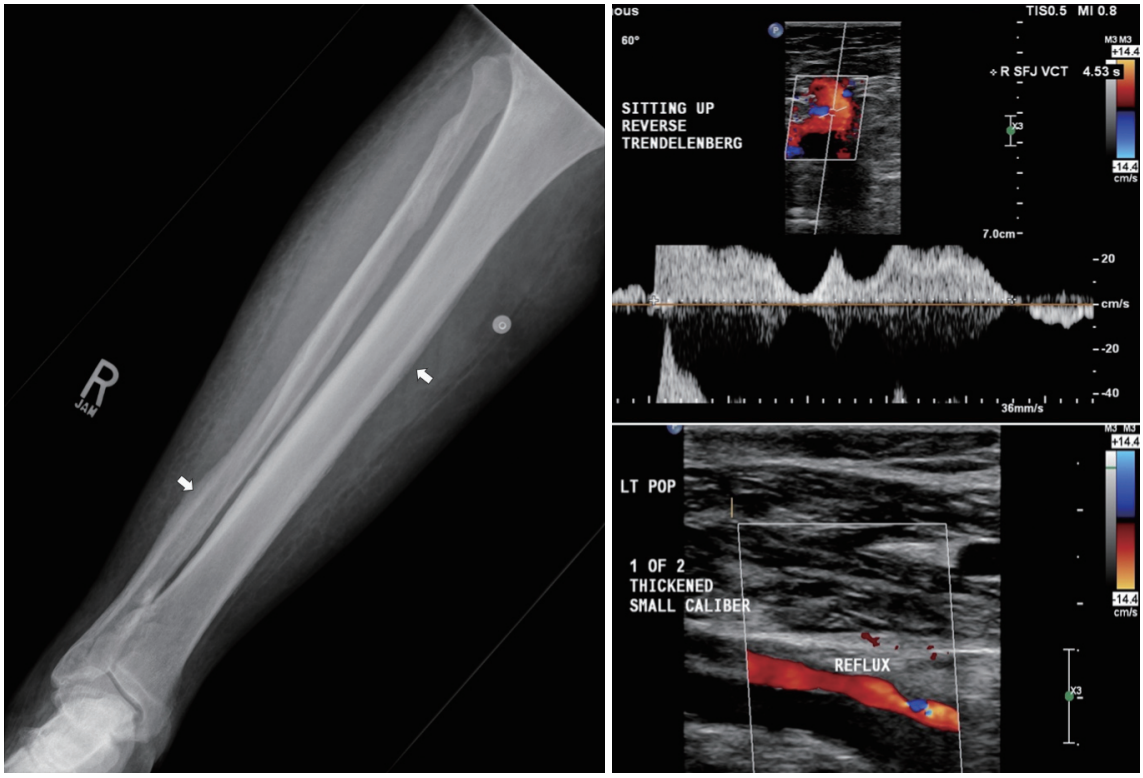

A B

Fig. 4. CVI in 77-year-old woman with history of lower extremity deep venous thrombosis, who presented with pain and swelling bilaterally in lower legs.
A. Anteroposterior radiograph of right lower leg revealing wavy and continuous periosteal reaction (arrows) in tibia and fibula. **B.** Color Doppler ultrasound revealing superficial venous reflux at right saphenofemoral junction (reflux time, 4.5 seconds after reverse Trendelenburg) and deep venous reflux at left popliteal vein.

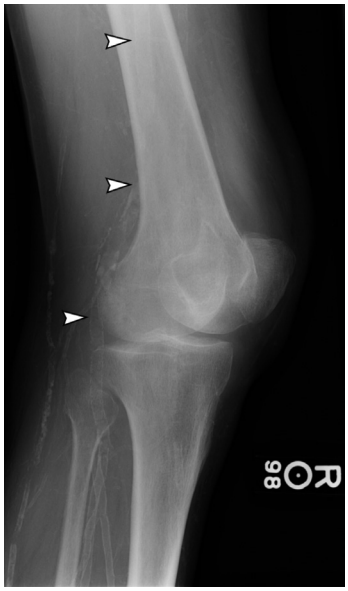

Fig. 5. Mönckeberg's arteriosclerosis in 70-year-old man with recent history of falling and knee pain. Lateral radiograph of knee revealing extensive calcification of femoral and popliteal arteries that appears with "railroad track" pattern (arrowheads), indicating Mönckeberg's arteriosclerosis.

Fig. 6. 57-year-old woman with phleboliths who presented with mass along lateral aspect of her right ankle. Radiograph of right ankle joint revealing soft tissue swelling with round nodular opacity within (arrowheads), showing phleboliths.

Korean Journal of Radiology
KJR

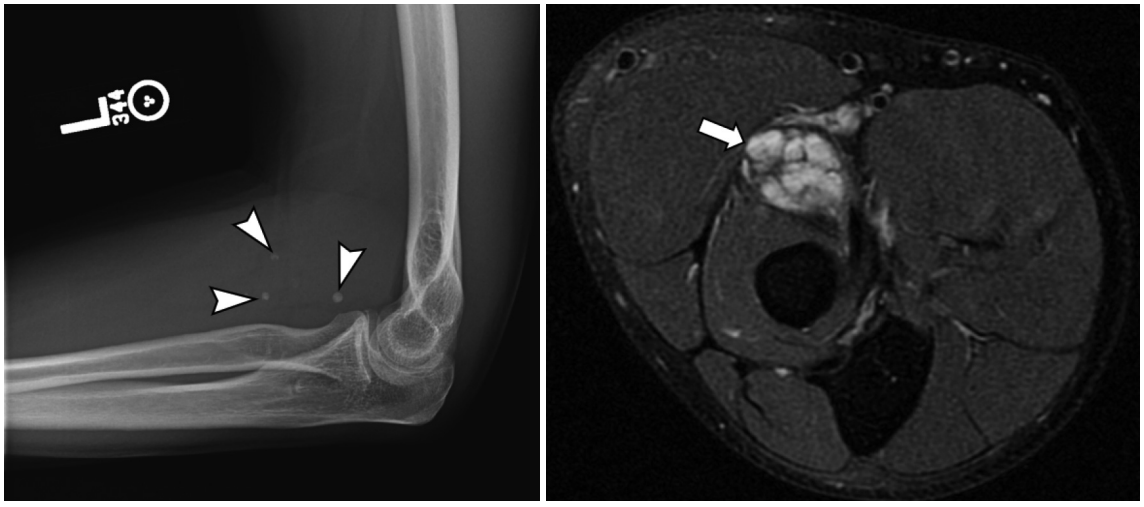

A B

Fig. 7. 38-year-old man with venous malformation who presented with fullness and mild pain in his left elbow.
A. Lateral radiograph revealing presence of phleboliths (arrowheads). **B.** Axial T2-weighted fat-saturated MR images demonstrating hyperintensity in tubular structures (arrow), which are discrete vessels, indicating venous malformation. MR = magnetic resonance

Fig. 8. Venous malformation in 17-year-old girl. She presented with hard mass in her lower right leg and 1-year history of walking pain. No trauma history was reported. Lateral radiograph revealing calcification (arrowheads) at posterior aspect of lower right extremity. Further MR imaging confirmed venous malformation (not shown).

hypointensity on T1-weighted images and increased signal intensity on T2-weighted images (Fig. 7). Heterogeneous signal intensity on T1-weighted images from hemorrhage or the presence of protein content is not uncommon (11). Marked diffuse enhancement of the slow-flowing venous channels on delayed postcontrast T1-weighted images is characteristic of venous malformation (11). Another helpful diagnostic clue is the presence of phleboliths (Figs. 7, 8) (11, 13).

Calcifications in Joint-Related Diseases

Calcium Pyrophosphate Dehydrate Deposition Disease

Calcium pyrophosphate dihydrate crystal deposition (CPPD) disease is defined as the deposition of CPPD crystals in hyaline cartilage, fibrocartilage, and other soft tissues inducing acute, subacute, or chronic inflammation (14). The knee joint accounts for the most (50–88%) cases, followed by the wrist (20%), and other areas including the ankle, hip, pubic symphysis, shoulder, and transverse ligaments of the spine (15). In the knee joint, disproportionate patellofemoral degenerative change is characteristic, and chondrocalcinosis involving the fibrocartilage menisci (Fig. 9) and hyaline cartilage is common (14, 16). In the wrist joint, calcification of the lunotriquetral ligament or the triangular fibrocartilage, associated with a narrowed radiocarpal joint space, is typically demonstrated. In addition, scapholunate advanced collapse is the most common form of wrist arthritis in patients with CPPD arthropathy (14). Additionally, narrowing of the metacarpophalangeal joints, sparing the interphalangeal joints, has been described.

A B C

Fig. 9. Calcium pyrophosphate dihydrate crystal doposition disease in 56-year-old woman who experienced chronic left knee pain and swelling for 1 day after minor fall.

A. Anteroposterior radiograph of knee revealing calcification at lateral aspect of tibiofemoral joint (arrow). **B.** Coronal computed tomography view revealing chondrocalcinosis at lateral meniscus (arrow). **C.** Sagittal computed tomography view revealing chondrocalcinosis situated at posterior horn of lateral meniscus (arrow).

A B

Fig. 10. TB trochanteric bursitis in 70-year-old man with left hip pain for 3 years.

A. Anteroposterior radiograph of left hip joint revealing bony destruction of greater trochanter and ossification in subgluteus medius bursa region (arrow). **B.** Coronal T1-weighted fat-suppressed post contrast images reveals marked enhancement of enlarged bursae with irregular, nodular-like synovia (arrowheads).

Tuberculous Trochanteric Bursitis

Extrapulmonary manifestations occur in approximately 20% of patients with tuberculous infection (17), and 1% to 3% of those with musculoskeletal system attributes. The most common osseous presentation is tuberculous spondylitis (18). The least commonly involved area is the extraspinal region (19), whereas peripheral arthritis accounts for 60% of cases, followed by osteomyelitis (38%), and tenosynovitis and bursitis (2%) (18). Tuberculous trochanteric bursitis can occur at any location via hematogenous spread; however, it more commonly involves the trochanteric (Fig. 10) and olecranon bursae (20). In the literature, the trochanteric bursae of the hip has the greatest prevalence (20, 21). Concomitant infection of both affected bursae and adjacent structures, such as bone and tendon, is not unusual. Isolated tuberculous trochanteric bursitis is associated with soft tissue swelling or minute flecks of calcification within the bursae in the early stages, followed by bone destruction (22).

Calcifications in Soft-Tissue-Related Diseases

Synovial Sarcoma

Synovial sarcoma accounts for 2.5% to 10.5% of all primary malignant soft-tissue neoplasms, the majority affecting the extremities (80–95%), especially in the popliteal fossa (23). It is reportedly the most common malignancy of the soft tissues of the foot and ankle in adolescents and young adults (23). Lesions are usually found adjacent to a joint. Histologically, synovial sarcoma is a malignant mesenchymal neoplasm composed of epithelial and spindle cell components (3, 23), and does not originate

Korean Journal of Radiology
KJR

from the synovium. It is categorized into three subtypes: biphasic, monophasic, and poorly differentiated (23). Synovial sarcoma commonly presents as a multilobulated lesion with cystic change, necrosis, and hemorrhage. Areas of hyalinization within the spindle cell components can form punctate calcifications in as many as 30% of the cases (3, 23). Radiographically, synovial sarcoma manifests as a juxta-articular soft-tissue mass with eccentric calcification (Fig. 11). Nonaggressive bone erosion, osteoporosis, and periosteal reaction have been illustrated, and these can easily be initially misdiagnosed as benign entities (3). On T1-weighted MR images, synovial sarcoma presents as an infiltrative, multilobulated soft-tissue mass with signal isointensity or mild hyperintensity compared with muscle. On T2-weighted MR images, a triple sign is apparent because of the intermixture of solid cellular elements (intermediate signal intensity), hemorrhage or necrosis (high signal intensity), and calcifications (low signal intensity) (23, 24). Marked heterogeneous enhancement after intravenous contrast administration is apparent in synovial sarcomas (Fig. 11).

Myositis Ossificans

Myositis ossificans is defined as a solitary calcified soft-tissue mass with heterotopic bone and cartilage formation, typically presenting in skeletal muscle (3, 25). Large muscles of the extremities account for 80% of cases (26). The mechanism of MO formation remains unclear, and the term "myositis" is a misnomer because there is no inflammatory process. MO usually results from injury, cerebrospinal disorders, or burns (3). These ossifying lesions are commonly surrounded by atrophic skeletal muscles with a distinct zone appearance. The lesion begins with an immature central nonossified cellular focus to the peripheral rim of mature lamellar bone (25). Radiographically, a faint calcification becomes apparent within 2 to 6 weeks of the onset of symptoms and progresses into a distinctive mass lesion with peripheral mature ossification after 6 to 8 weeks (Fig. 12).

Parasitic Infection (Cysticercosis)

Cysticercosis is a common parasitic infection caused by the dissemination of Taenia solium from the intestine to the systemic organs by drinking contaminated water or ingesting uncooked pork. The most commonly affected organs are subcutaneous tissues, skeletal muscles, lungs, brain, eyes, liver and, occasionally, the heart (27). Typical radiographic features are rice-grain calcifications

A B

Fig. 11. Synovial sarcoma in 54-year-old man with palpable mass in his right foot.
A. Anteroposterior radiograph of foot revealing calcified soft-tissue mass (arrow) between second and third proximal phalanges with extrinsic bone erosions. **B.** Axial T1-weighted fat-suppressed post-contrast images demonstrating heterogeneous enhancement of mass lesion (arrowheads), which dorsally extended between second and third proximal phalanges. Low signal intensity changes within lesion indicate calcification.

parallel to the long axis of the soft tissue (Fig. 13). These calcifications are dead larval cysts (cysticerci) (28). In addition, intramuscular abscesses, subcutaneous nodules, or pseudohypertrophy of the muscles have been described (29).

Connective Tissue Disease (Scleroderma)

Calcinosis circumscripta manifests as dense, white dermal plaques or subcutaneous nodules usually identified near a joint (Fig. 14) (3). These calcifications are commonly

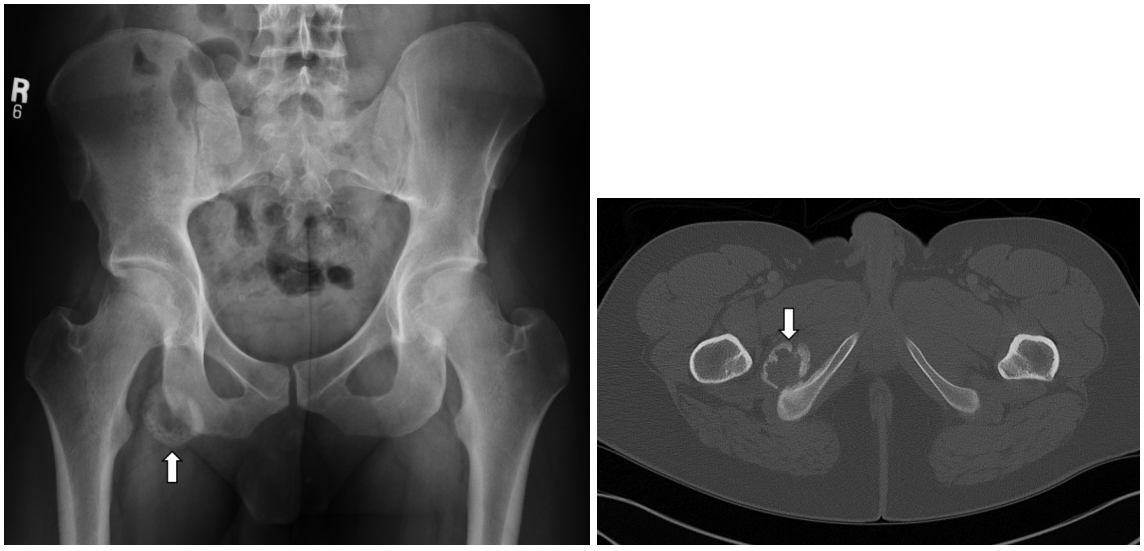

Fig. 12. Mature MO in 28-year-old man with 3-month history of hamstring injury, who presented with right groin pain.
A. Anteroposterior radiograph of pelvis revealing well-circumscribed ossified mass (arrow) located proximally in soft tissue of right thigh. **B.** Axial computed tomography view revealing distinct margin of lesion with peripheral mature ossification (arrow) within right adductor magnus muscle.

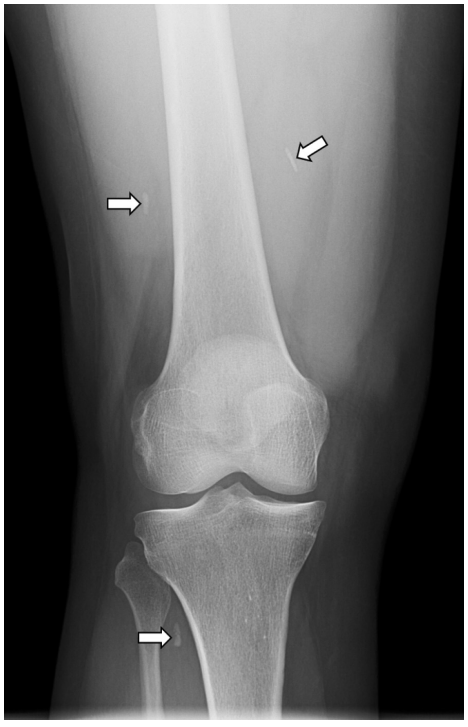

Fig. 13. 51-year-old South American woman with cysticercosis infection who presented with right knee pain. Anteroposterior radiograph of right knee revealing typical rice-grain calcification (arrows) in distal muscles of right femur and calf, characteristic of cysticercosis infection.

Fig. 14. Scleroderma in 71-year-old woman presenting with left hand pain. Anteroposterior radiograph of left hand revealing multiple dense and well-defined calcified nodules (arrowheads) in soft tissues of first to fourth phalanges, confirming her medical history of scleroderma.

Korean Journal of Radiology
KJR

associated with connective tissue diseases including the early stages of polymyositis, dermatomyositis, systemic lupus erythematosus, progressive systemic sclerosis, scleroderma and calcinosis, Raynaud phenomenon, esophageal dysmotility, sclerodactyly, and telangiectasia (CREST) syndrome (3).

Calcifications in Tendon/Ligament-Related Diseases

Degenerative Calcification

The Achilles tendon is composed of the tendons of the soleus and gastrocnemius muscles, and inserts at the posterior calcaneal tuberosity. It is enclosed within a paratendon rather than a synovial sheath (30). Ossification of the Achilles tendon is an uncommon complication of Achilles tendon injury and is usually the result of previous trauma (tendon rupture or repeated micro-trauma) or surgery (31). Based on the anatomical ossification sites on radiographs, the disorder is classified into 3 types. In type 1, ossification is located at the tendinous insertion. In type 2, it is located 1–3 cm from the tendon insertion (Fig. 15). Finally, in type 3, lesions are localized up to 12 cm from tendon insertion. Lesions can further be grouped into those with partial ossification and those with complete ossification of the tendon (31, 32).

Fig. 15. 70-year-old man with degenerative calcification of Achilles tendon, who injured his Achilles tendon 20 years previously. Lateral radiograph of left ankle joint revealing partial ossification (arrowheads) of Achilles tendon, type 2, confirming degenerative calcification.

Calcific Tendinitis

Calcific tendinitis is defined as deposition of calcium hydroxyapatite crystals within the tendons. It most commonly occurs in individuals between 30 and 60 years of age, and women are slightly predominant among those diagnosed (33). It primarily affects the shoulder and hip joints. In the shoulder joint, the supraspinatus tendon (Fig. 16) is involved in 80% of cases, followed by the infraspinatus, which accounts for 15%, and the subscapularis tendons, which account for 5% (34). Radiographically, calcification, which is restricted to the tendon without evidence of degenerative joint disease, is diagnostic (35). During the calcification phase, the deposit appears to be homogeneously dense and well-defined, whereas in the resorptive phase, it can manifest as fluffy and ill-defined (33, 35).

Pellegrini-Stieda Lesion/Syndrome

Pellegrini-Stieda syndrome is characterized by ossification of the femoral attachment of the medial collateral ligament,

Fig. 16. Calcific tendinitis in 45-year-old woman with left shoulder pain. Anteroposterior radiograph of left shoulder joint revealing calcification (arrow) with ill-defined margin located at insertion of supraspinatus tendon, suggestive of resorptive phase of calcific tendinitis.

and develops adjacent to the medial femoral epicondyle 3 or 4 weeks following injury (36). Clinical presentations include medial swelling of the knee with pain; however, sometimes the patient is asymptomatic. On radiographs, a linear vertical ossification is depicted adjacent to medial femoral condyle (Fig. 17). However, this ossification can also involve the adductor magnus tendon.

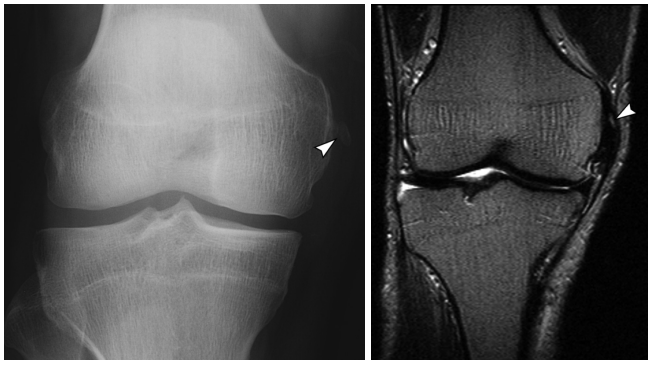

A B

Fig. 17. Pellegrini-Stieda syndrome in 60-year-old woman with right knee pain.
A. Anteroposterior radiograph of right knee of revealing linear calcification (arrowhead) abutting medial femoral condyle. **B.** Coronal T2-weighted MR images confirming lesion is situated in region of proximal attachment of medial collateral ligament (arrowhead).

Fig. 18. Injection granulomas in 69-year-old woman.
Radiograph revealing multiple foci of calcifications (arrows) superimposed bilaterally over buttocks.

Iatrogenic Calcifications (Injection Granulomas)

Injection granulomas result from repeated injections into the subcutaneous fat (37). They are usually found in the upper outer quadrant of the gluteal regions but can occur at any injection site. Tissue reactions depend on the site, number of injections, and the composition of the injected material (38). On radiographs, injection granulomas are characterized by well-circumscribed calcified nodules (Fig. 18) (39).

Metastatic Calcifications

Causes of metastatic calcifications include chronic renal failure, hyperparathyroidism, pseudohypoparathyroidism, sarcoidosis, and tophaceous gout.

Chronic Renal Failure

Biochemical disturbances resulting from chronic renal failure can give rise to vascular and soft-tissue metastatic calcifications (40). Clinically, these patients exhibit hyperparathyroidism secondary to chronic renal failure and

Fig. 19. Uremic tumoral calcinosis in 56-year-old woman who presented with palpable mass at right elbow. Anteroposterior radiograph of elbow joint revealing multilobulated, rounded, calcified lesions (arrowhead) in soft tissues located at medial aspect of her elbow, indicating uremic tumoral calcinosis.

Korean Journal of Radiology
KJR

hemodialysis (Figs. 19-21). These calcified lesions, however, cannot be distinguished from primary tumoral calcinosis based on imaging findings or histology (3, 41).

Primary Hyperparathyroidism

When parathyroid hormone is autonomously secreted, primary hyperparathyroidism can result in bone resorption when this secretion is not suppressed by elevated serum levels of calcium (42). It is most commonly encountered in individuals > 50 years of age, and in women more than men, by a factor of three- to fourthfold (43). In approximately 90% of cases, they are caused by parathyroid adenomas and, in approximately 10%, they result from multi-gland hyperplasia. In extremely rare cases, primary hyperparathyroidism results from parathyroid carcinomas (44). Skeletal manifestations of hyperparathyroidism include subperiosteal bone resorption, a "salt-and-pepper" appearance of skull demineralization, distal clavicle tapering, and brown tumors (43). Subperiosteal bone resorption usually begins at the radial aspects of the middle phalanges of the middle and index fingers, and at the distal phalangeal tufts as acro-osteolysis (Fig. 22) (42).

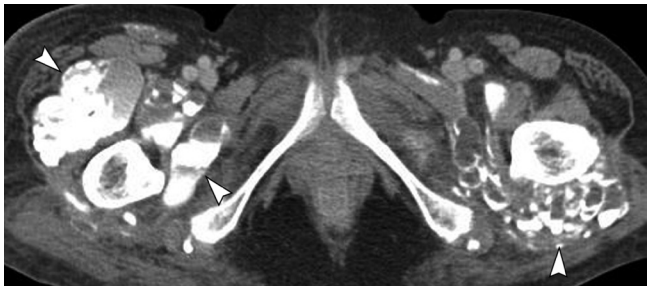

Fig. 20. Uremic tumoral calcinosis in 55-year-old woman with bilateral palpable painless masses in buttocks. Axial computed tomography scan reveals multilobulated calcified cystic lesions with sedimentation (arrowheads) at greater trochanteric bursa (bilaterally), which are indistinguishable from primary tumoral calcinosis.

Pseudohypoparathyroidism

Pseudohypoparathyroidism is a heterogeneous group of disorders characterized by end-organ resistance to parathyroid hormone. It is subclassified into types Ia, Ib, Ic, and II (45). Albright's hereditary osteodystrophy is a clinical entity described together with pseudohypoparathyroidism, presenting as brachydactyly, rounded face, short stature, central obesity, subcutaneous ossifications, and varying degrees of intellectual disability (46). Brachydactyly typically manifests as a shortening of the third, fourth, and fifth metacarpals, and the first distal phalanx (Fig. 23).

A B

Fig. 21. Uremic tumoral calcinosis in 43-year-old woman with chronic renal failure who had undergone hemodialysis for 6 years and presented with 2-month history of palpable mass in her right gluteal region.
A. Anteroposterior radiograph of pelvis revealing massive periarticular calcinosis (arrowheads) abutting right hip joint, which is indistinguishable from primary tumoral calcinosis. **B.** Coronal T2-weighted MR image revealing heterogeneous intensity of calcinosis (arrowheads).

Sarcoidosis

Sarcoidosis is a systemic granulomatous disease characterized by noncaseating granulomas in soft tissues without definite cause. The disease most commonly affects the lungs, lymph nodes, skin, and eyes (47). However, it can also involve the musculoskeletal system, in which 1% to 13% (estimated average, 5%) of sarcoidosis cases have been reported (48). Approximately 90% of the osseous lesions found in sarcoidosis are small bone lesions,

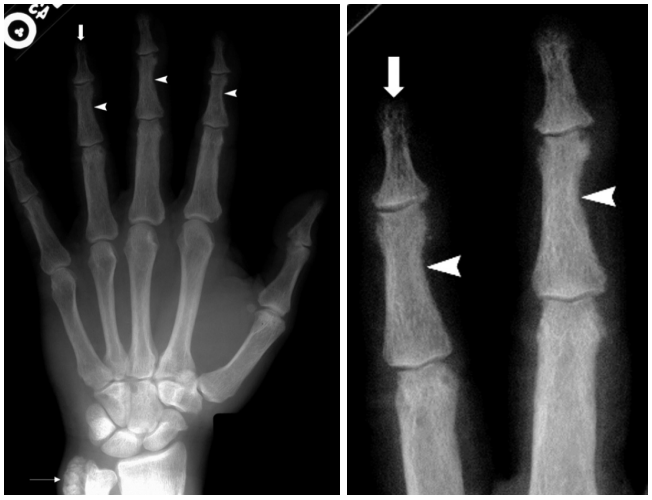

A B

Fig. 22. Hyperparathyroidism in 47-year-old woman who presented with hand pain.
A. Anteroposterior radiograph of right hand reveals subperiosteal bone resorption along radial aspects of middle phalanges of second, third, and fourth fingers (arrowheads). Thin-arrow identifies lobulated calcified mass abutting right ulna. **B.** Magnification view reveals bone erosion of distal phalangeal tufts, resulting in acro-osteolysis (arrow). Arrowheads shows subperiosteal bone resorption.

Fig. 23. Pseudohypoparathyroidism in 22-year-old woman with short stature and intellectual disability. Anteroposterior radiograph of left hand revealing shortened first, fourth, and fifth metacarpal bones (arrowheads) with calcification adjacent to fourth metacarpal bone.

A B

Fig. 24. Type 3 sarcoid dactylitis in 51-year-old woman with right hand pain.
Anteroposterior **(A)**, and lateral **(B)** radiograph of right hand demonstrating radiolucent lesions with "lace-like" patterns at proximal and middle phalanx of third digit (arrowheads), and fusiform thickening of infiltrated soft tissue (arrows) resulting from sarcoid dactylitis.

Fig. 25. Gout in 82-year-old man with right foot pain.
Anteroposterior radiograph of right foot demonstrating radiopaque lesion (gouty tophus) with juxta-articular erosion and soft tissue swelling at first metatarsophalangeal joint (arrow). Note that joint space and bone density are normal, with absence of intra-articular erosions.

Korean Journal of Radiology
KJR

especially in the distal and the middle phalanges of the second and third digits (49). Classically, they present with a "lacy" lytic appearance (47), or with extensive bone erosion and pathological fractures, sparing the articular surfaces (50). In addition, the infiltrated soft tissues will also demonstrate "sausage finger" or "radish" deformities (49). A single bone can exhibit up to 3 types of small bone lesions (49): type 1, large bone geodes or bullous lesions; type 2, multiple well demarcated, rounded, and occasionally confluent geodes located in the heads of the phalanges; and type 3, a "lace-like" pattern with thickened bone sheets and a thin cortex (Fig. 24).

Tophaceous Gout

Gouty arthritis is caused by deposition of monosodium urate monohydrate crystals and subsequently forms periarticular tophus masses that can induce both acute and chronic inflammation (3). Adjacent soft tissue swelling due to gouty tophus deposition is virtually diagnostic on radiographs. Gouty arthritis typically exhibits juxta-articular, marginal erosion with an overhanging edge and extends perpendicularly from underlying bone. The first metatarsophalangeal joint of the foot is the most commonly affected (Fig. 25).

CONCLUSION

Soft-tissue calcifications are not uncommon findings in daily imaging. By systematically using the distribution pattern of the calcified lesions, additional laboratory testing, and clinical history, appropriate differential diagnoses can be approached.

REFERENCES

1. Santili C, Akkari M, Waisberg G, Kessler C, Alcantara Td, Delai PL. Calcinosis universalis: a rare diagnosis. *J Pediatr Orthop B* 2005;14:294-298
2. Abdallah-Lotf M, Grasland A, Vinceneux P, Sigal-Grinberg M. Regression of cutis calcinosis with diltiazem in adult dermatomyositis. *Eur J Dermatol* 2005;15:102-104
3. Olsen KM, Chew FS. Tumoral calcinosis: pearls, polemics, and alternative possibilities. *Radiographics* 2006;26:871-885
4. Chander S, Gordon P. Soft tissue and subcutaneous calcification in connective tissue diseases. *Curr Opin Rheumatol* 2012;24:158-164
5. Stewart VL, Herling P, Dalinka MK. Calcification in soft tissues. *JAMA* 1983;250:78-81
6. Lafferty FW, Reynolds ES, Pearson OH. Tumoral calcinosis: a metabolic disease of obscure etiology. *Am J Med* 1965;38:105-118
7. Tokoro S, Satoh T, Okubo Y, Igawa K, Yokozeki H. Latent dystrophic subcutaneous calcification in patients with chronic venous insufficiency. *Acta Derm Venereol* 2009;89:505-508
8. Rana RS, Wu JS, Eisenberg RL. Periosteal reaction. *AJR Am J Roentgenol* 2009;193:W259-W272
9. Kim H, Greenberg JS, Javitt MC. Breast calcifications due to Mönckeberg medial calcific sclerosis. *Radiographics* 1999;19:1401-1403
10. Tahmasbi-Arashlow M, Barghan S, Kashtwari D, Nair MK. Radiographic manifestations of Mönckeberg arteriosclerosis in the head and neck region. *Imaging Sci Dent* 2016;46:53-56
11. Flors L, Leiva-Salinas C, Maged IM, Norton PT, Matsumoto AH, Angle JF, et al. MR imaging of soft-tissue vascular malformations: diagnosis, classification, and therapy follow-up. *Radiographics* 2011;31:1321-1340; discussion 1340-1341
12. Fayad LM, Hazirolan T, Bluemke D, Mitchell S. Vascular malformations in the extremities: emphasis on MR imaging features that guide treatment options. *Skeletal Radiol* 2006;35:127-137
13. Ernemann U, Kramer U, Miller S, Bisdas S, Rebmann H, Breuninger H, et al. Current concepts in the classification, diagnosis and treatment of vascular anomalies. *Eur J Radiol* 2010;75:2-11
14. Steinbach LS, Resnick D. Calcium pyrophosphate dihydrate crystal deposition disease revisited. *Radiology* 1996;200:1-9
15. Ogata M. [A clinical study of calcium pyrophosphate dihydrate crystal deposition disease]. *Nihon Seikeigeka Gakkai Zasshi* 1985;59:819-834
16. Jacobson JA, Girish G, Jiang Y, Sabb BJ. Radiographic evaluation of arthritis: degenerative joint disease and variations. *Radiology* 2008;248:737-747
17. Westall J. Tuberculosis levelling off worldwide. *BMJ* 1997;314:921
18. De Backer AI, Vanhoenacker FM, Sanghvi DA. Imaging features of extraaxial musculoskeletal tuberculosis. *Indian J Radiol Imaging* 2009;19:176-186
19. Hugosson C, Nyman RS, Brismar J, Larsson SG, Lindahl S, Lundstedt C. Imaging of tuberculosis. V. Peripheral osteoarticular and soft-tissue tuberculosis. *Acta Radiol* 1996;37:512-516
20. Jaovisidha S, Chen C, Ryu KN, Siriwongpairat P, Pekanan P, Sartoris DJ, et al. Tuberculous tenosynovitis and bursitis: imaging findings in 21 cases. *Radiology* 1996;201:507-513
21. Meyerding HW, Mroz RJ. Tuberculosis of the greater trochanter. *JAMA* 1933;101:1308-1313
22. Rehm-Graves S, Weinstein AJ, Calabrese LH, Cook SA, Boumphrey FR. Tuberculosis of the greater trochanteric bursa. *Arthritis Rheum* 1983;26:77-81
23. Murphey MD, Gibson MS, Jennings BT, Crespo-Rodríguez AM, Fanburg-Smith J, Gajewski DA. From the archives of the AFIP: imaging of synovial sarcoma with radiologic-pathologic

correlation. *Radiographics* 2006;26:1543-1565
24. Jones BC, Sundaram M, Kransdorf MJ. Synovial sarcoma: MR imaging findings in 34 patients. *AJR Am J Roentgenol* 1993;161:827-830
25. Kransdorf MJ, Meis JM. From the archives of the AFIP. Extraskeletal osseous and cartilaginous tumors of the extremities. *Radiographics* 1993;13:853-884
26. Nuovo MA, Norman A, Chumas J, Ackerman LV. Myositis ossificans with atypical clinical, radiographic, or pathologic findings: a review of 23 cases. *Skeletal Radiol* 1992;21:87-101
27. Bhalla A, Sood A, Sachdev A, Varma V. Disseminated cysticercosis: a case report and review of the literature. *J Med Case Rep* 2008;2:137
28. Roche CJ, O'Keeffe DP, Lee WK, Duddalwar VA, Torreggiani WC, Curtis JM. Selections from the buffet of food signs in radiology. *Radiographics* 2002;22:1369-1384
29. Naik D, Srinath M, Kumar A. Soft tissue cysticercosis - Ultrasonographic spectrum of the disease. *Indian J Radiol Imaging* 2011;21:60-62
30. Narváez JA, Narváez J, Ortega R, Aguilera C, Sánchez A, Andía E. Painful heel: MR imaging findings. *Radiographics* 2000;20:333-352
31. Richards PJ, Braid JC, Carmont MR, Maffulli N. Achilles tendon ossification: pathology, imaging and aetiology. *Disabil Rehabil* 2008;30:1651-1665
32. Morris KL, Giacopelli JA, Granoff D. Classifications of radiopaque lesions of the tendo Achillis. *J Foot Surg* 1990;29:533-542
33. Speed CA, Hazleman BL. Calcific tendinitis of the shoulder. *N Engl J Med* 1999;340:1582-1584
34. Serafini G, Sconfienza LM, Lacelli F, Silvestri E, Aliprandi A, Sardanelli F. Rotator cuff calcific tendonitis: short-term and 10-year outcomes after two-needle us-guided percutaneous treatment--nonrandomized controlled trial. *Radiology* 2009;252:157-164
35. ViGario GD, Keats TE. Localization of calcific deposits in the shoulder. *Am J Roentgenol Radium Ther Nucl Med* 1970;108:806-811
36. Mendes LF, Pretterklieber ML, Cho JH, Garcia GM, Resnick DL, Chung CB. Pellegrini-Stieda disease: a heterogeneous disorder not synonymous with ossification/calcification of the tibial collateral ligament-anatomic and imaging investigation. *Skeletal Radiol* 2006;35:916-922
37. Cockshott WP, Thompson GT, Howlett LJ, Seeley ET. Intramuscular or intralipomatous injections? *N Engl J Med* 1982;307:356-358
38. Prosch H, Mirzaei S, Oschatz E, Strasser G, Huber M, Mostbeck G. Case report: gluteal injection site granulomas: false positive finding on FDG-PET in patients with non-small cell lung cancer. *Br J Radiol* 2005;78:758-761
39. Stein L, Elsayes KM, Wagner-Bartak N. Subcutaneous abdominal wall masses: radiological reasoning. *AJR Am J Roentgenol* 2012;198:W146-W151
40. Degrassi F, Quaia E, Martingano P, Cavallaro M, Cova MA. Imaging of haemodialysis: renal and extrarenal findings. *Insights Imaging* 2015;6:309-321
41. Gordon LF, Arger PH, Dalinka MK, Coleman BG. Computed tomography in soft tissue calcification layering. *J Comput Assist Tomogr* 1984;8:71-73
42. Chang CY, Rosenthal DI, Mitchell DM, Handa A, Kattapuram SV, Huang AJ. Imaging findings of metabolic bone disease. *Radiographics* 2016;36:1871-1887
43. Khan AA, Hanley DA, Rizzoli R, Bollerslev J, Young JE, Rejnmark L, et al. Primary hyperparathyroidism: review and recommendations on evaluation, diagnosis, and management. A Canadian and international consensus. *Osteoporos Int* 2017;28:1-19
44. Khan A, Bilezikian J. Primary hyperparathyroidism: pathophysiology and impact on bone. *CMAJ* 2000;163:184-187
45. Wilson LC, Hall CM. Albright's hereditary osteodystrophy and pseudohypoparathyroidism. *Semin Musculoskelet Radiol* 2002;6:273-283
46. Mantovani G. Clinical review: pseudohypoparathyroidism: diagnosis and treatment. *J Clin Endocrinol Metab* 2011;96:3020-3030
47. Moore SL, Teirstein AE. Musculoskeletal sarcoidosis: spectrum of appearances at MR imaging. *Radiographics* 2003;23:1389-1399
48. James DG, Neville E, Carstairs LS. Bone and joint sarcoidosis. *Semin Arthritis Rheum* 1976;6:53-81
49. Aptel S, Lecocq-Teixeira S, Olivier P, Regent D, Teixeira PG, Blum A. Multimodality evaluation of musculoskeletal sarcoidosis: imaging findings and literature review. *Diagn Interv Imaging* 2016;97:5-18
50. Koyama T, Ueda H, Togashi K, Umeoka S, Kataoka M, Nagai S. Radiologic manifestations of sarcoidosis in various organs. *Radiographics* 2004;24:87-104